ChemComm

Accepted Manuscript

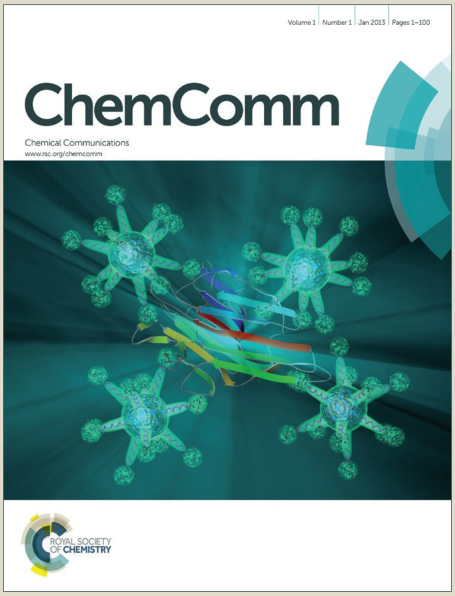

ROYAL SOCIETY OF CHEMISTRY

www.rsc.org/chemcomm

ChemComm

COMMUNICATION

Reactive Atmospheric Pressure Plasma for Highly Efficient Removal of Structure-Directing Agents from Zeolite Thin Films

Received 00th January 20xx,
Accepted 00th January 20xx

DOI: 10.1039/x0xx00000x

www.rsc.org/

H.-T. Chien[a], M.-c. Chen[a], P.-S. Huang[a], J.-Y. Lai[b,c], C.-C. Hsu[a,]* and D.-Y. Kang[a,]*

We present a novel approach to remove the structure-directing agent (SDA) from as-synthesized zeolites using an atmospheric pressure plasma jet (APPJ). This reduces the time required to less than 60 seconds as compared to the exsiting themal calcination, whose durations range from hours to days. The highly reactive plasma also results in a pronounced Q^3-to-Q^4 transformation in the pure-silica zeolite MFI.

Zeolites are crystalline microporous aluminosicates and one of the best-known molecular sieves. These materials have been widely applied in molecular separation,[1-4] catalysis,[5-7] and low-k dielectric materials.[8-10] The synthesis of zeolites typically requires a structure-directing agent (SDA) to guide the assembly pathways in forming specific types of micropores.[11-14] Zeolites synthesized using SDA require the removal of SDA in order to create microporous voids (Fig. 1).

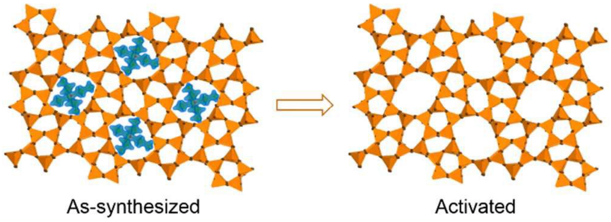

Fig. 1. Schematic illustration of process used in removal of SDA from as-synthesized zeolites for activation of micropores

The most common and reliable method used in the removal of SDA is thermal calcination, in which as-synthesized zeolites are thermally treated at 400 to 600°C to combust organic compounds for durations ranging from hours to days.[15-17] This process is energy-intensive and time-consuming and the high temperatures involved can have a detrimental effect on materials with a low-temperature stability, such as polymeric substrates for the growth of zeolite membranes.[18-20] Furthermore, toxic gasses, such as nitrogen oxide, may also be generated during the calcination process.

These limitations in the conventional approach to calcination have led to the development of new methods for the removal of SDA. One method involves extraction, in which SDA is transferred from micropores within the zeolites to a solvent.[21-24] However, the size of SDA molecules is nearly identical to that of the microporous voids, such that short-range interactions occur between SDA and the framework of the zeolite.[25] Both of these phenomena tend to hinder the extraction process. One modification to this approach has been developed using degradable SDA to improve extraction efficiency; however, this still requires more than 20 hr to achieve the complete removal of SDA.[26] Low-temperature treatment using ozone[27] or dielectric-barrier discharge (DBD) plasma[28] have also been reported; however, detailed results demonstrating the absence of SDA following treatment are scarce. A cold plasma treatment method has been developed for the same purpose; however, this requires a multiple-step treatment process using various types of plasma.[29] A UV-assisted method has also been investigated as a means to expedite thermal calcination.[30] Nevertheless, this process still requires high temperatures (425 °C) and leads to unexpected methylation on the surface of zeolites. Researchers have investigated synthesis without the use of SDA; however, these methods generally involve a tradeoff with regard to synthesis time, yield, or product purity.[31-33]

Herein, we report a novel approach to the removal of SDA from zeolite thin films using an atmospheric pressure plasma jet (APPJ), for use in material synthesis and processing.[34-37] The setup of the proposed APPJ system is presented in Fig. 2. It has been hypothesized that the reactive species generated in the nitrogen APPJ readily reacts with the SDA, resulting in defragmentation, which allows the removal of the SDA by convective flow from the APPJ.[38-40] Pure-silica zeolite MFI was selected as a model system for this study.

---

[a] Department of Chemical Engineering, National Taiwan University, Taipei 10617, Taiwan. E-mails: dunyen@ntu.edu.tw; chsu@ntu.edu.tw
[b] Department of Chemical Engineering, Chung Yuan Christian University, Taoyuan City 32023, Taiwan.
[c] R&D Center for Membrane Technology, Chung Yuan Christian University, Taoyuan City 32023, Taiwan.

Electronic Supplementary Information (ESI) available: Experimental details, a larger spectral region of FT-IR spectra of various thin films, top- and side-view SEM images of thin film samples, and raw images of contact angle measurements on bare and modified films. See DOI: 10.1039/x0xx00000x

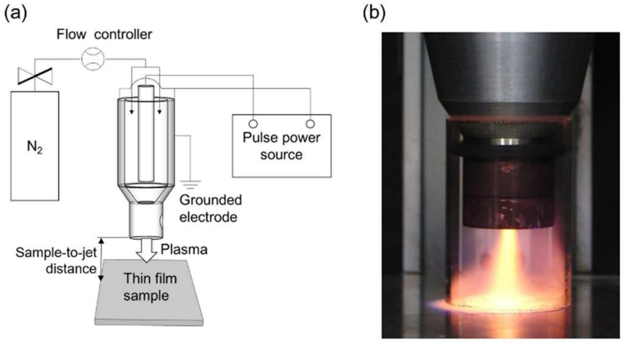

Fig. 2. (a) Schematic illustration of APPJ setup and (b) photographs of a treatment process using APPJ

A number of solid-state characterization techniques were used to investigate the micromorphology of the thin films. Controlled experiments with calcined zeolite MFI thin films were also performed for comparison with the APPJ-treated samples. Post-calcination and post-APPJ-treatment surface modification were conducted to elucidate the surface activity (Q^3/Q^4 ratio) associated with various approaches to SDA removal.

Zeolite MFI thin films with a thickness of approximately 300 nm were cast on silicon wafer substrates. The as-synthesized thin films were then subjected to thermal calcination or APPJ treatment with various sample-to-jet distances and process durations. Thin film samples that underwent APPJ treatment with a jet-to-sample distance of 1mm for 20 seconds were denoted as 1mm-20s; the denotations of the rest of the samples can be deduced by analogy. FT-IR spectra in a region of 1250 to 4000 cm^{-1} and with a larger spectral region are presented in the *Supplementary information* (Fig. S1). A comparison of FT-IR spectra between as-synthesized and thermally calcined samples suggests that absorption values between 1250 to 1700 cm^{-1} and between 2800 to 3000 cm^{-1} are associated with organic compounds, including tetrapropylammonium hydroxide (TPAOH) as SDA and TWEEN® 80 used for stabilizing the casting solution. Absorption between 2800 to 3000 cm^{-1} in particular can be assigned to C-H stretching, whereas absorption between 2800 to 3000 cm^{-1} can be attributed to various vibrational modes in TPAOH and TWEEN® 80. No noticeable difference in FT-IR spectra was observed between the calcined and APPJ-treated samples. This qualitatively suggests that the effects of APPJ treatment over a period of 60 seconds are comparable to those of thermal calcination over a period of 5 hours. Furthermore, the FT-IR spectra taken near the center of the thin films (Fig. S1b) were nearly identical to those taken near the edge of the same samples (Fig. S1c), which suggested the APPJ uniformly treated the entire thin film samples. Quantitative measurement involved elemental analysis using energy dispersive X-ray spectroscopy (EDS). The deduced carbon/silicon intensities for the various thin film samples are summarized in Fig. 3a, and the raw spectra are presented in the *Supplementary information* (Fig. S2). All of the spectra were obtained from frontal measurements of the thin films, which is representative of the bulk (rather than just the surface) properties due to the fact that the penetration distance of EDS is more than 1 μm,[41, 42] which exceeds the thickness of the thin film. Among all of the measured samples, the as-synthesized pure-silica zeolite MFI thin films presented the highest carbon/silicon intensity, due to the presence of TPAOH and TWEEN® 80. Among APPJ-treated samples, the carbon/silicon intensity monotonically decreased with the duration of treatment. The carbon/silicon intensity in samples with sample-to-jet distances of 1 and 3 mm treated for over 20 seconds is lower than that observed in the calcined thin films. The same results were observed in the 5mm-60s sample. This implies that within 60 seconds, APPJ treatment removes more SDA than thermal calcination does over a period of 5 hours.

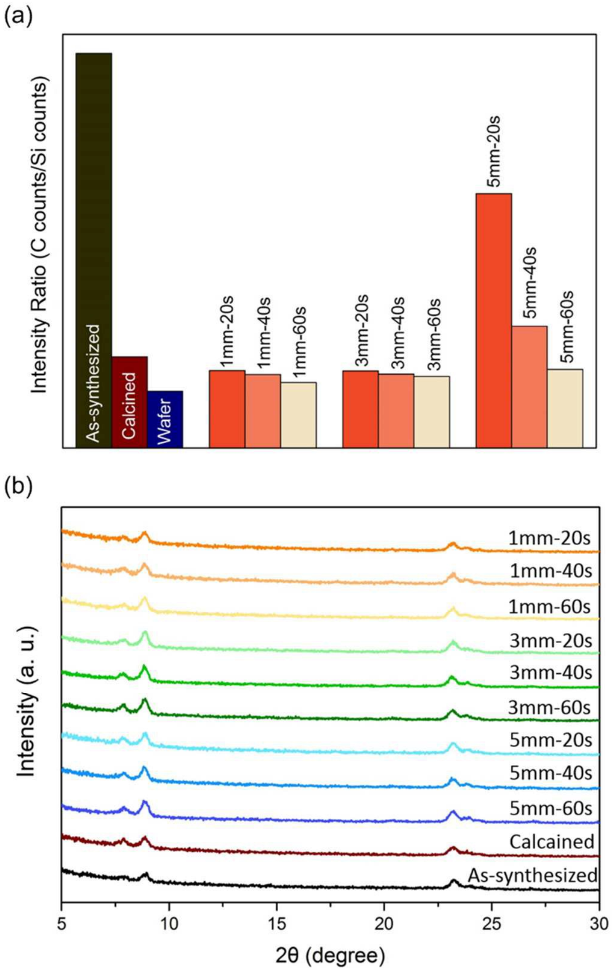

Fig. 3. (a) Silicon/carbon intensity derived from energy dispersive X-ray spectra for as-synthesized, calcined, and APPJ-treated zeolite MFI thin films and bare silicon wafers. (b) GIXRD patterns of as-synthesized, calcined, and APPJ-treated zeolite MFI thin films.

Grazing-incidence X-ray diffraction (GIXRD) analysis was performed to assess the crystallinity of pure-silica zeolite MFI thin films (Fig. 3b). Typical zeolite MFI diffraction patterns were observed in the as-synthesized as well as calcined samples. The contrast in GIXRD images of the calcined thin film exceeds that of the as-synthesized samples, very likely due to higher electron density in the calcined thin films resulting from the creation of micropores. All of the APPJ-treated samples were nearly identical with regard to GIXRD patterns. FT-IR and EDS analysis suggest that the topology of the zeolite MFI was preserved, even after APPJ treatment, despite the fact that just as much of the SDA was removed by this process as by calcination. Top- and side-view SEM images of the as-synthesized, calcined, and APPJ-treated (60 seconds) samples are presented in the *Supplementary information* (Fig. S3 and S4). No significant differences were observed between the calcined and the APPJ-treated zeolite MFI thin films, which is in consistent with the results obtained from GIXRD measurements.

To elucidate changes (at the molecular level) in silicon species of APPJ-treated MFI thin films, we used triethoxy(octyl)silane to perform surface modification of as-synthesized, calcined, and APPJ-treated films. In pure-silica zeolite MFI, Q^3 and Q^4 are the major silicon species.[43-46] Notation Q^n represents a silicon species with *n* bridging oxygen atoms bound to other silicon atoms. Thus, Q^4 silicon atoms are not adjacent to any hydroxyl group, whereas Q^3 silicon atoms are bound to a hydroxyl group and considered reactive. The surface modifier, triethoxy(octyl)silane, is expected to graft to the external surface of the MFI crystal due to the fact that it is too bulky to enter the micropores of the MFI, the pore size of which is less than 6Å. The modifier probes the Q^3/Q^4 ratio in various zeolite thin film samples. FI-IR spectroscopy performed in ATR mode was used for the characteriziation of surface functionality following modification. The FT-IR spectra of as-synthesized, calcined, and APPJ-treated (60 seconds) samples are presented in Fig. 4a. The as-synthesized thin film presented higher absorption in the C-H stretching region (2800-3000 cm^{-1}) than did the calcined sample. There are two reasons for this. First, the calcined zeolite MFI possesses a lower Q^3/Q^4 ratio than does the as-synthesized zeolite, which allows the immobilization of more triethoxy(octyl)silane. Second, the as-synthesized zeolite MFI contains both TPAOH and TWEEN® 80 in addition to the grafted triethoxy(octyl)silane, which contributes to an absorption between 2800 to 3000 cm^{-1}. Compared to the calcined samples, absorption between 2800 to 3000 cm^{-1} in the APPJ-treated samples was shown to decrease monotonically with the sample-to-jet distance. This suggests that a shorter sample-to-jet distance during APPJ treatment would result in a lower Q^3/Q^4 ratio in the pure-silica zeolite MFI.

Contact angle measurements with water were performed on the bare and modified samples. We expected that the silane modifier would react with the silanol at Q^3 species, thereby making the surface more hydrophobic due to the long alkyl chain on triethoxy(octyl)silane. The deduced contact angles are summarized in Fig. 4b and the raw images of the measurements are presented in the *Supplementary information* (Fig. S5). The contact angles of all bare thin film samples were fairly similar prior to surface modification. This can be attributed to the fact that Q^3 and Q^4 species possess similar hydrophilicity. The as-synthesized zeolite MFI thin film presented the largest difference in contact angle before and after surface modification, suggesting that it may have the highest Q^3/Q^4 ratio among all of the tested samples. The difference in contact angle before and after surface modification decreased in the following order: calcined thin film > 5mm-60s > 3mm-60s > 1mm-60s. The FT-IR characterization and contact angle measurements both suggest that APPJ treatment had a more pronounced effect on Q^3-to-Q^4 conversion than did thermal calcination. A greater effect on Q^3-to-Q^4 conversion indicates that APPJ treatment is better able to facilitate the condensation of adjacent silanols than is thermal calcination. We propose that the far shorter treatment time and pronounced Q^3-to-Q^4 conversion is a result of synergy between the temperature and reactivity of the APPJ.[47] The surface temperature of samples during plasma jet treatment was 400-500 °C.[40] It is well known that a great number of reactive species exist in plasma and the nitrogen APPJ used in this work includes a large number of excited nitrogen molecules,[47] possessing energy levels exceeding 6 eV above the ground state. The quenching of these excited molecules provides energy sufficient for the removal of SDA and adjacent silanol condensation. The synergetic effect of the moderate temperature and reactivity resulted in the rapid activation of the zeolite thin films. The Q^4 type silicon atom is more stable (less reactive) than the Q^3 silicon atom. Therefore the zeolite samples treated by APPJ, as compared to the calcined samples, are more suitable for applications such as separations under harsh conditions.

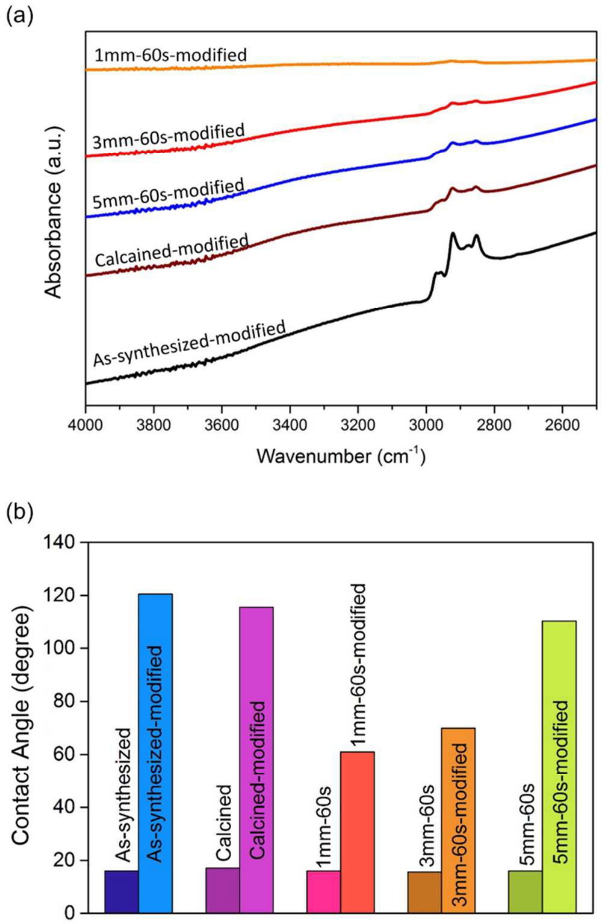

Fig. 4. (a) FT-IR spectra of as-synthesized, calcined, and APPJ treated thin film samples following surface modification with triethoxy(octyl)silane. (b) Comparison of as-synthesized, calcined, and APPJ treated thin film samples with regard to contact angle of water before and after surface modification.

In conclusion, this study demonstrated the effectiveness of atmospheric pressure plasma jet (APPJ) for the removal of organic structure-directing agent (SDA) in zeolites, reducing the time required for processing from several hours using thermal calcination to just tens of seconds. FT-IR and EDS signals of organic species in pure-silica zeolite thin films that underwent APPJ treatment for 60 seconds were as low as those of calcined films. Furthermore, our results indicate that the lower Q^3/Q^4 ratio in the APPJ-treated samples is comparable to that of the thermally-calcined thin film. These findings indicate that APPJ treatment has a stronger effect on Q^3-to-Q^4 transformation than does thermal calcination. With minor modifications, the proposed APPJ treatment would be applicable to zeolite thin films in a variety of configurations, such as hollow fiber form, and zeolite pellets. This time- and energy-saving technique greatly facilitates the application of zeolitic materials in large-scale devices and processes.

D.-Y.K. acknowledges financial support from the Ministry of Science and Technology (MOST) of Taiwan (NSC102-2218-E-002-015-MY2 and MOST 104-2218-E-002-006h). C.-C.H. acknowledges support from MOST, Taiwan (103-2221-E-002-184-MY3). The authors are grateful to Kai-Hsin Liou for assistance on the artwork of the table of contents entry.

Notes and references

1. Z. Lai, G. Bonilla, I. Diaz, J. G. Nery, K. Sujaoti, M. A. Amat, E. Kokkoli, O. Terasaki, R. W. Thompson, M. Tsapatsis and D. G. Vlachos, *Science*, 2003, **300**, 456-460.
2. T. C. Bowen, R. D. Noble and J. L. Falconer, *J. Membr. Sci.*, 2004, **245**, 1-33.
3. M. A. Snyder and M. Tsapatsis, *Angew. Chem. Int. Ed.*, 2007, **46**, 7560-7573.
4. J. Caro and M. Noack, *Microporous Mesoporous Mater.*, 2008, **115**, 215-233.
5. S. Heng, K. L. Yeung, M. Djafer and J.-C. Schrotter, *J. Membr. Sci.*, 2007, **289**, 67-75.
6. A. J. Jones, R. T. Carr, S. I. Zones and E. Iglesia, *J. Catal.*, 2014, **312**, 58-68.
7. M. Choi, K. Na, J. Kim, Y. Sakamoto, O. Terasaki and R. Ryoo, *Nature*, 2009, **461**, 246-249.
8. H.-Y. Lu, C.-L. Teng, C.-H. Kung and B.-Z. Wan, *Ind. Eng. Chem. Res.*, 2011, **50**, 3265-3273.
9. Z. B. Wang, A. Mitra, H. T. Wang, L. M. Huang and Y. Yan, *Adv. Mater.*, 2001, **13**, 1463-1466.
10. S. Li, Z. Li and Y. Yan, *Adv. Mater.*, 2003, **15**, 1528-1531.
11. C. S. Cundy and P. A. Cox, *Chem. Rev.*, 2003, **103**, 663-702.
12. R. Simancas, D. Dari, N. Velamazán, M. T. Navarro, A. Cantín, J. L. Jordá, G. Sastre, A. Corma and F. Rey, *Science*, 2010, **330**, 1219-1222.
13. T. Wakihara and T. Okubo, *Chem. Lett.*, 2005, **34**, 276-281.
14. H. Chen, J. Wydra, X. Zhang, P.-S. Lee, Z. Wang, W. Fan and M. Tsapatsis, *J. Am. Chem. Soc.*, 2011, **133**, 12390-12393.
15. M. E. Davis and R. F. Lobo, *Chem. Mater.*, 1992, **4**, 756-768.
16. C. S. Cundy and P. A. Cox, *Microporous Mesoporous Mater.*, 2005, **82**, 1-78.
17. L. Tosheva and V. P. Valtchev, *Chem. Mater.*, 2005, **17**, 2494-2513.
18. M. Zhou, X. Liu, B. Zhang and H. Zhu, *Langmuir*, 2008, **24**, 11942-11946.
19. M. Severance, B. Wang, K. Ramasubramanian, L. Zhao, W. S. W. Ho and P. K. Dutta, *Langmuir*, 2014, **30**, 6929-6937.
20. B. Zhang, M. Zhou and X. Liu, *Adv. Mater.*, 2008, **20**, 2183-2189.
21. C. W. Jones, K. Tsuji, T. Takewaki, L. W. Beck and M. E. Davis, *Microporous Mesoporous Mater.* 2001, **48**, 57-64.
22. H. Wang, B. A. Holmberg and Y. Yan, *J. Mater. Chem.*, 2002, **12**, 3640-3643.
23. C. W. Jones, K. Tsuji and M. E. Davis, *Nature*, 1998, **393**, 52-54.
24. T. Takewaki, L. W. Beck and M. E. Davis, *J. Phys. Chem. B*, 1999, **103**, 2674-2679.
25. S. L. Burkett and M. E. Davis, *J. Phys. Chem.*, 1994, **98**, 4647-4653.
26. H. Lee, S. I. Zones and M. E. Davis, *J. Phys. Chem. B*, 2005, **109**, 2187-2191.
27. S. Heng, P. P. S. Lau, K. L. Yeung, M. Djafer and J.-C. Schrotter, *J. Membr. Sci.*, 2004, **243**, 69-78.
28. Y. Liu, Y.-x. Pan, P. Kuai and C.-j. Liu, *Catal. lett.*, 2010, **135**, 241-245.
29. M. El Roz, L. Lakiss, V. Valtchev, S. Mintova and F. Thibault-Starzyk, *Microporous Mesoporous Mater.*, 2012, **158**, 148-154.
30. S. Eslava, F. Iacopi, M. R. Baklanov, C. E. A. Kirschhock, K. Maex and J. A. Martens, *J. Am. Chem. Soc.*, 2007, **129**, 9288-9289.
31. M. Pan and Y. S. Lin, *Microporous Mesoporous Mater.*, 2001, **43**, 319-327.
32. S. D. Kim, S. H. Noh, J. W. Park and W. J. Kim, *Microporous Mesoporous Mater.*, 2006, **92**, 181-188.
33. N. Ren, J. Bronić, B. Subotić, X.-C. Lv, Z.-J. Yang and Y. Tang, *Microporous Mesoporous Mater.*, 2011, **139**, 197-206.
34. J.-H. Im, J.-H. Lee and D.-W. Park, *Surf. Coat. Tech.*, 2008, **202**, 5471-5475.
35. D. Kolacyak, J. Ihde, C. Merten, A. Hartwig and U. Lommatzsch, *J. Colloid Interface Sci.*, 2011, **359**, 311-317.
36. Y.-S. Lin, T.-H. Tsai and S.-W. Tien, *Thin Solid Films*, 2013, **529**, 248-252.
37. S.-M. Chang, E. F. Rodríguez Tolava, Y.-J. Yang, H.-C. Li, R.-C. Lee, N.-L. Wu and C.-C. Hsu, *J. Am. Ceram. Soc.*, 2014, **97**, 708-712.
38. A. N. Wright and C. A. Winkler, *Active Nitrogen*, Academic Press, New York, 1968.
39. H. Chang, C.-M. Hsu, P.-K. Kao, Y.-J. Yang, C.-C. Hsu, I. C. Cheng and J.-Z. Chen, *J. Power Sources*, 2014, **251**, 215-221.
40. H. Chang, Y.-J. Yang, H.-C. Li, C.-C. Hsu, I. C. Cheng and J.-Z. Chen, *J. Power Sources*, 2013, **234**, 16-22.
41. H. C. Vallet, *Appl Phys A*, 1997, **65**, 387-394.
42. B. Gilbert, B. H. Frazer, F. Naab, J. Fournelle, J. W. Valley and G. De Stasio, *Am. Mineral.*, 2003, **88**, 763-769.
43. S. L. Burkett and M. E. Davis, *Chem. Mater.*, 1995, **7**, 920-928.
44. S. P. Naik, A. S. T. Chiang, R. W. Thompson, F. C. Huang and H.-M. Kao, *Microporous Mesoporous Mater.*, 2003, **60**, 213-224.

45. C.-H. Cheng, T.-H. Bae, B. A. McCool, R. R. Chance, S. Nair and C. W. Jones, *J. Phys. Chem. C*, 2008, **112**, 3543-3551.
46. M. H. Kassaee, D. S. Sholl and S. Nair, *J. Phys. Chem. C*, 2011, **115**, 19640-19646.
47. Y.-w. Hsu, Y.-j. Yang, C.-y. Wu and C.-c. Hsu, *Plasma Chem. Plasma Process.*, 2010, **30**, 363-372.